Emma McGregor[1]
Lee Kempster[1]
Robin Wait[2]
Sandy Y. Welson[2]
Martin Gosling[1]
Michael J. Dunn[3]
Janet T. Powell[1, 4]

[1]Department of Vascular Surgery, Imperial College School of Medicine, Charing Cross Hospital, London, UK
[2]Kennedy Institute of Rheumatology Division, Imperial College School of Medicine, London, UK
[3]Department of Cardiothoracic Surgery, National Heart and Lung Institute, Imperial College School of Medicine, Heart Science Centre, Harefield Hospital, Middlesex, UK
[4]University Hospitals of Coventry and Warwickshire, Coventry, UK

Identification and mapping of human saphenous vein medial smooth muscle proteins by two-dimensional polyacrylamide gel electrophoresis

Changing smooth muscle phenotype and abnormal cell proliferation are important features of vascular pathology, including the failure of saphenous vein bypass grafts. We have characterised and mapped protein expression in human saphenous vein medial smooth muscle, using two-dimensional (2-D) polyacrylamide gel electrophoresis. The 2-D system comprised a nonlinear immobilised pH 3–10 gradient in the first dimension (separating proteins with isoelectric point values between pH 3–10), and 12%T total gel concentration sodium dodecyl sulphate polyacrylamide gel electrophoresis in the second dimension (separating proteins in the range 14 000–200 000 Daltons). Using a combination of peptide mass fingerprinting by matrix-assisted laser desorption/ionisation-time of flight mass spectrometry and partial amino acid sequencing by nanospray tandem mass spectrometry, a subset of 149 protein spots was analysed, with 129 protein spots being identified and mapped. The data presented here are an important addition to the limited knowledge of venous medial smooth muscle protein expression *in vivo*. Our protein map will facilitate the identification of proteins differentially expressed in human saphenous vein bypass grafts. In turn, this may lead to the elucidation of molecular events involved in saphenous vein bypass graft failure. The map should also provide a basis for comparative studies of protein expression in vascular smooth muscle of varying origins.

Keywords: Human saphenous vein / Vascular smooth muscle / Bypass grafting / Two-dimensional polyacrylamide gel electrophoresis / Matrix-assisted laser desorption/ionization-time of flight mass spectrometry PRO 0116

1 Introduction

Vein bypass grafting using human saphenous vein (HSV) remains the most commonly used method to bypass occluded vessels, since HSV is readily accessed, relatively plentiful, easily harvested [1] and provides adequate flow to the recipient artery. Saphenous vein bypass surgery depends on the successful adaptation of the vessel to high pressure and pulsatile flow of the arterial circulation. However, the tendency of venous bypass grafts to occlude is an important drawback, emphasising the problems which may arise when vein is transposed into the arterial circulation. During the first year after coronary artery bypass surgery up to 15% of venous grafts occlude [2]. In the first year after femoropopliteal bypass surgery up to 28% of venous grafts occlude [3]. Migration of smooth muscle cells into the intima, with alteration to a synthetic, proliferative phenotype, causing intimal hyperplasia, is an important underlying cause of vein graft failure [2, 4]. Similar cellular changes are observed following angioplasty of diseased arteries. Superficially, it might appear important to characterise the protein expression of smooth muscle cells cultured from different vessels to investigate phenotypic variability and phenotypic switching. However, cultured smooth muscle cells are not contractile and exhibit a phenotype very different from the smooth muscle embedded in the connective tissue of the medial layer of blood vessels. The structure of saphenous vein lends itself to straightforward dissection of the medial smooth muscle layer away from the adventitia. The main advantage of using intact medial smooth muscle tissue is an enriched source of smooth muscle cells that retain a contractile phenotype. However, a consequence of using dissected intact tissue is contamination by other cell types, *e.g.* endothelial and red blood cells in the case of medial smooth muscle. Little is known about the initiating factors leading to the development of intimal hyperplasia. 2-D PAGE is therefore an ideal technique to exploit in order to investigate protein expression, post-translational modification, function and regulation in vein graft disease.

The aim of this study was to generate a reference protein map that would facilitate the identification of proteins differentially expressed in HSV bypass grafts. Here we pre-

Correspondence: Dr. Emma McGregor, Proteome Sciences plc, South Wing Laboratory, Institute of Psychiatry, KCL, De Crespigny Park, London SE5 8 AF, UK
E-mail: E.McGregor@iop.kcl.ac.uk
Fax: +44-207-848-5114

Abbreviation: HSV, human saphenous vein

 1615-9853/01/1111–1405 $17.50+.50/0

sent the first map of HSV medial smooth muscle protein expression, mapping 149 distinct proteins, of which 129 are identified. Our long-term goal is to establish a reference database of HSV medial smooth muscle protein expression, which could be used to progress our understanding of the molecular events involved in saphenous vein bypass graft failure.

2 Materials and methods

2.1 Human saphenous vein samples

Saphenous vein was harvested from patients undergoing aortocoronary or infrainguinal bypass, or high ligation of saphenous vein for correction of varicose veins, and immediately brought to the laboratory in M199 media (Life Technologies, Paisley, UK) containing penicillin (50 U/mL) and streptomycin (50 μg/mL) (Sigma, Poole, UK). The Riverside Research Ethics Committee approved the use of saphenous vein for the investigations discussed in this report.

2.2 Medial dissection from human saphenous vein

Connective tissue was removed from sections of vein (1–2 cm) and the lumen opened longitudinally. Endothelium was removed by scraping the opened lumen with a scalpel and washing with PBS, pH 7.2. Using forceps the media was peeled from the adventitia. Dissected tissue was immediately frozen between aluminium tongs (precooled in liquid N_2) and samples stored at –70°C prior to preparation for 2-DE or was preserved in formalin (10% formaldehyde), pH 7, prior to immunohistochemistry.

2.3 Immunohistochemical validation of medial dissections

Dissected media for immunostaining was set in paraffin blocks and sectioned (4 μm thickness) on a base sledge microtome (Leitz Wetzlar). Immunohistochemistry was performed using the avidin-biotin complex (ABC) method [5]. Consecutive sections from the same medial dissection were incubated with monoclonal antibodies specific for smooth muscle markers, alpha smooth muscle actin (dilution 1:400) and smooth muscle myosin (dilution 1:250), both obtained from Sigma. Sections were also incubated with a monoclonal antibody specific for the endothelial cell marker, CD-31 (dilution 1:50) (Serotec, Oxford, UK). A biotinylated secondary antibody (rabbit antimouse IgG) (Vector, Peterborough, UK) was used at a 1:100 dilution. Staining was visualised by development with DAB (3, 3'-diamino-benzidine-tetrahydrochloride) (Vector).

2.4 Preparation of tissue samples

Sample preparation was performed according to Weekes *et al*. [6] and Heinke *et al*. [7]. Briefly, frozen tissue samples (70–110 mg) were pulverised under liquid N_2 into a fine powder using a pestle and mortar. The resulting powder was collected, homogenised in lysis buffer (9.5 M urea, 2% w/v CHAPS, 0.8% w/v Pharmalyte, pH 3–10, and 1% w/v DTT), in 1.5 mL Eppendorf tubes, (for preparative and analytical gels, 150 μL of lysis buffer was added to 10 mg wet weight of tissue), sonicated at 4°C for 5 min and centrifuged at 13 000 *g* at 20°C for 1 h. The supernatant was harvested and protein concentration was determined [6] using a modification of the method described by Bradford [8]. Solubilised protein samples were divided into 50 μL aliquots and stored at –70°C.

2.5 2-D PAGE

2-D PAGE was performed according to Weekes *et al.* [6] and Heinke *et al.* [7]. IEF was performed using 180 mm, immobilised, nonlinear pH gradient strips (IPG DryStrips) of pH 3–10 (Amersham Pharmacia Biotech, Uppsala, Sweden). For preparative gels a protein load of 400 μg was applied to each IPG strip using an in-gel rehydration method, as described by Rabilloud *et al.* [9] and Sanchez *et al.*, [10]. Samples were diluted in rehydration solution (8 M urea, 0.5% w/v CHAPS, 0.2% w/v DTT and 0.2% w/v Pharmalyte) pH 3–10 and rehydrated overnight in a reswelling tray (Amersham Pharmacia Biotech). Strips were focussed at 0.05 mA/IPG strip for 60 kVh at 20°C [11]. Once IEF was completed the strips were equilibrated in 6 M urea containing 30% v/v glycerol, 2% w/v SDS and 0.01% w/v Bromophenol blue, with the addition of 1% w/v DTT for 15 min, followed by the same buffer without DTT, but with the addition of 4.8% w/v iodoacetamide for 15 min [12]. SDS-PAGE was performed using 12%T, 2.6%C separating polyacrylamide gels without a stacking gel, using the Hoefer DALT system [13]. The second dimension was carried out overnight at 20 mA/gel at 8°C and was terminated when the Bromophenol dye front had migrated off the lower end of the gels.

2.6 Protein visualisation

After electrophoresis, preparative 2-D gels were fixed for a minimum of 1 h in a methanol:acetic acid:water solution (4:1:5 v/v/v). 2-D protein profiles were visualised by silver staining using the PlusOne silver staining kit (Amersham Pharmacia Biotech) with slight modifications to ensure compatibility with subsequent MS analysis [14]. Analytical gels were fixed and silver stained in the same way but without modifications.

2.7 Sample preparation for MS

Protein spots were excised with a 2 mm diameter round cutter. Multiple cores were taken from weakly stained spots, and in some cases corresponding proteins were pooled from several gels. In-gel trypsin digestion was performed according to published methods [15–17] modified for use with a robotic digestion system (Genomic Solutions Investigator ProGest, Huntington, UK). Gel pieces were destained by washing with 30 μL of 15 mM potassium ferricyanide/50 mM sodium thiosulphate [18] followed by three washes with 100 μL Milli-Q H_2O (Millipore, Bedford, MA, USA). Cysteine residues were reduced with DTT and were derivatized with iodoacetamide. Gel pieces were then dehydrated with acetonitrile, dried at 60°C and reswollen with 10 μL digestion buffer (containing modified trypsin, 6.5 ng/μL) (Promega, Madison, WI, USA) in 25 mM ammonium hydrogen carbonate. After 8 h incubation at 37°C, products were recovered by sequential extractions with 25 mM ammonium hydrogen carbonate, 5% v/v formic acid, and acetonitrile. Extracts were lyophilized, resuspended in 20 μL of 0.1% v/v TFA / 10% v/v acetonitrile, and 0.5 μL aliquots were removed for MALDI analysis. Extracts for ESI-MS were desalted on Millipore Ziptips, according to the manufacturers instructions.

2.8 MALDI-MS

MALDI-MS was performed using a Micromass TofSpec 2E spectrometer (Manchester, UK), equipped with a 337 nm nitrogen laser. The instrument was operated in the positive ion reflectron mode at 20 kV accelerating voltage with time-lag focusing. The matrix was a mixture of α-cyano-4-hydroxy-cinnamic acid and nitrocellulose and was applied as a microcrystalline thin film by a modification of the procedure of Vorm and Mann [19]. Aliquots (0.5 μL) of the digest solution were deposited on the matrix film, allowed to dry and were desalted by brief washing with a few microlitres of 0.1% v/v TFA. Spectra were internally calibrated using trypsin autolysis products, and the resulting peptide masses were searched against a local copy of the nonredundant database maintained by the National Centre for Biotechnology Information (http://www.ncbi.nlm.nih.gov) using the Protein Probe search engine (Micromass). Where necessary additional searches were performed using the programs Mascot [20] or ProFound (http://prowl.rockefeller.edu) [21]. An initial mass tolerance of 50 ppm was used in all searches.

2.9 ESI-MS

Desalted samples were dissolved in 1–2 μL of 50% v/v methanol/0.1% v/v aqueous formic acid, loaded into palladium coated borosilicate nanoelectrospray needles (Protana, Odense, Denmark), and mounted in the source of a Micromass Q-Tof hybrid quadrupole/orthogonal acceleration time of flight spectrometer. Stable electrospray was obtained at capillary voltages between 900 and 1200 V. The collision gas was argon, and collision energies and argon pressure were tuned to optimise the fragmentation pattern of individual precursor ions. Daughter ion spectra were charge-state de-encrypted and de-isotoped using a proprietary maximum entropy algorithm (MaxEnt 3, Micromass), and amino acid sequences were manually deduced with the assistance of Micromass's peptide sequencing program PepSeq. The resulting sequences were searched against NCBI's nonredundant database using BLAST [22].

2.10 Computer analysis

Silver stained gels were scanned at 100 μm resolution using a Molecular Dynamics Personal SI Laser Densitometer (Sunnyvale, CA, USA). Protein spots were analysed qualitatively using the PDQuest 2-D software V 6.2.0 (Bio-Rad, Hercules, CA, USA). Briefly, background and vertical streaks were removed from each gel image and spots digitised by Gaussian fit, giving rise to a synthetic image. In order for PDQuest to carry out automatic determination of observed p*I* and M_r values, it was first necessary to calibrate the digitised image for these parameters. The length of the first dimension was divided into 10% sections. The pH value at each division was then interpolated from a published Amersham Pharmacia Biotech pH gradient plot which describes pH as a function of distance for a pH 3–10 nonlinear gradient [23]. Protein spots were chosen that represented the full range of pH and p*I* values assigned according to the above calculation. To calibrate for M_r, protein spots that migrated in line with Rainbow molecular weight markers (Amersham Pharmacia, Biotech) were chosen and these values assigned accordingly.

3 Results and discussion

In this study we present a 2-D electrophoretic map of protein expression from the medial (smooth muscle cell) layer of human saphenous vein (HSV). Tissue identity was confirmed by immunohistochemistry, using antibodies specific to smooth muscle markers, alpha smooth muscle actin and smooth muscle myosin, performed on sections of dissected saphenous vein medial smooth muscle (data not shown). The absence of contaminating endothelial cells was confirmed using an endothelial cell marker-specific antibody, CD-31 (data not shown).

Protein extraction was performed using two different lysis buffers and compared for efficiency of extraction. Tissue samples were prepared as in Section 2.4. Samples were lysed in standard lysis buffer (9.5 M urea, 2% w/v CHAPS, 0.8% w/v Pharmalyte, pH 3–10, and 1% w/v DTT) (n = 6), or in a second choice of lysis buffer containing 5 M urea, 2 M thiourea, 2% w/v CHAPS, 2% v/v sulphobetaine 3–10, 2 mM TBP (n = 6) [24]. Protein extraction was more efficient using standard lysis buffer, 1.3 ± 0.3 mg/mL of protein (n = 6), than using the second choice of lysis buffer, 1.0 ± 0.2 mg/mL (n = 6), p = 0.038 (unpaired Students t-test). Therefore, the urea/thiourea extracts were not processed further.

Protein spots were separated from vein samples emanating from three separate patients. Gels (pH 3–10) had 130985.05, 236563.25 and 117534.1, valid spot quantities respectively, according to PDQuest 2-D software and spot patterns of gels were highly reproducible between samples (data not shown). The protein spots excised for sequencing were present in all three gels.

The 2-D PAGE map of HSV medial smooth muscle protein expression consists of protein spots ranging from molecular mass of 11 000 to 200 000 Da and p*I* of pH 3 to 10 (Fig. 1). A subset of 149 protein spots have been analysed by MALDI-MS, and identifications assigned to 129

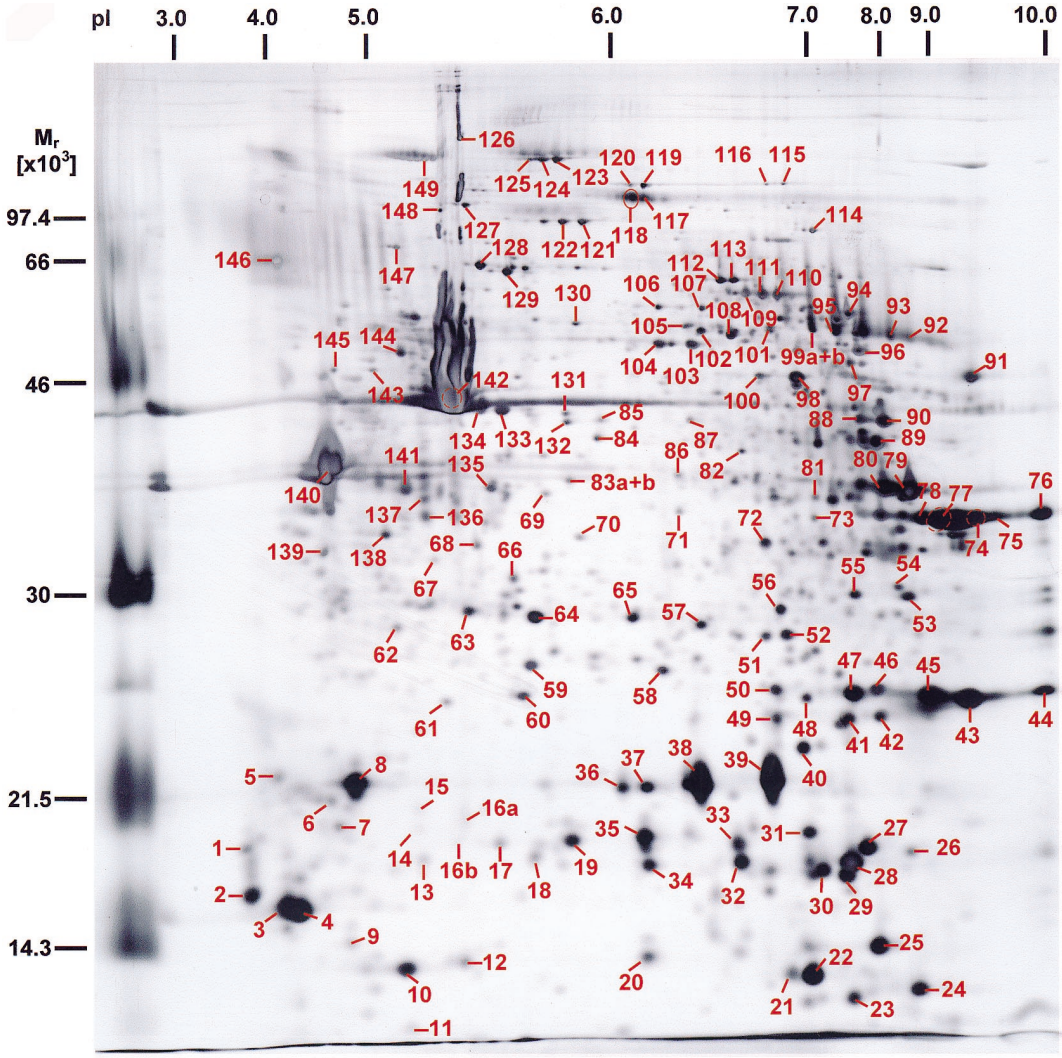

Figure 1. 2-D PAGE map of human saphenous vein medial smooth muscle proteins. Proteins (400 μg loading) were separated by IEF using 180 mm, immobilised, nonlinear pH gradient strips (IPG DryStrips) of pH 3–10, followed by 12%T gradient SDS-PAGE gels. Proteins were visualised by silver staining. Spot numbers refer to numbers in Table 1. Proteins were identified by MALDI- MS and nanospray-MS.

(Table 1). Twenty protein spots were unable to be identified. Where required, nanospray MS was used to further confirm protein identity by partial amino acid sequencing.

Arterialisation of saphenous vein bypass grafts is associated with the development of intimal hyperplasia (migration of smooth muscle cells into the intima, cell proliferation and establishment of a dense connective tissue matrix), which can cause graft occlusion. These well-described histological changes represent the chronic adaptation of saphenous vein to the arterial circulation.

Several of the identified spots have been characterised previously in smooth muscle using 2-D PAGE. Calponin (spots 74–78) and SM22α (spots 19, 25, 32–36, 38, 39, 41, 43–45, 47,) expression was investigated in avian and mammalian smooth muscle during smooth muscle differentiation, with multiple isoforms of each being expressed [25]. Our results are in keeping with this pattern of expression, with protein spot location in the gel being similar. Other proteins such as myosin light chain (spots 3 and 4) have also been investigated in smooth muscle by 2-D PAGE [26].

Actin-fibre remodelling is an early event in the adaptation of saphenous vein to arterial haemodynamics. Therefore, potential proteins of interest that would be pertinent to the adaptation of human saphenous vein to arterial flow, would be cytoskeletal proteins *e.g.* actin fibres, and actin depolymerising factors *e.g.* gelsolin. After exposure to arterial haemodynamics one might expect changes in the expression /regulation of these proteins.

Fifteen spots ranging from a molecular mass of 14 400 to 26 300 Da and a p*I* of 5.78 to 9.90 were identified as the actin binding protein SM22α (theoretical M_r/p*I* 22500 Da/8.88). Spots 43–45 suggest isoelectric isoforms of this protein. Gimona and colleagues [25] have reported several such isoforms in chicken gizzard and porcine stomach smooth muscle. However, the average molecular mass of these isoforms is 26 000 Da. Spots 36, 38, and 39 form a chain of isoelectric isoforms closely matching the theoretical molecular weight of SM22α, but exhibit a more acidic nature (p*I* 6.00–6.64). Spots 19, 25, and 32–35 with molecular mass ranging from 14 400 to 19 000 Da probably represent proteolytic fragments. The range of p*I* values of these spots may also indicate this. Spots 41 and 47 may represent aggregation of proteolytic fragments, due to their larger molecular masses.

Spots 74–78 were identified as calponin (theoretical mass/p*I* 33 200 Da/9.14), a protein with high sequence homology to SM22α [27, 28]. The spots form an isoform chain in a similar manner to SM22α. Gimona *et al.* have also reported the existence of such calponin isoforms [25]. Charge trains in 2-DE are normally associated with post-translational modifications such as acetylation and phosphorylation. Both SM22α and calponin are subject to phosphorylation *in vitro*. However, neither protein is phosphorylated *in vivo* [25]. The possibility of other modifications resulting in charge train formations cannot be ruled out.

Spots 121 and 122 were identified as gelsolin, a human actin depolymerization factor (theoretical mass/p*I* 85 700 Da/5.90). Gelsolin is a Ca^{2+}- and polyphosphoinositide 4,5-bisphosphate (PIP_2)[1]-regulated actin filament severing and capping protein that is implicated in actin remodelling in growing and in apoptotic cells [29]. It is the most potent actin filament severing protein identified to date [30]. Observed molecular masses of these spots were 93 700 and 94 100 Da, respectively. However, resolution of large molecular weight proteins by 2-DE is relatively poor and so some artefactual discrepancies may occur. Nevertheless, spots 121 and 122 appear to be members of a charge train increasing in acidity. This may be indicative of phosphorylation and indeed it has been shown that actin depolymerization factor may be regulated by pathways including phosphorylation [31]. Other actin binding proteins identified include filamin, spots 117 and 118, and F-actin capping protein, spot 69.

Spots 84, 85, 126, 131 and 132 were identified as smooth muscle α-actin 3 (theoretical mass/p*I* 41 900 Da/5.31). The average observed molecular weight of spots 84, 85, 131 and 132 agreed approximately with the theoretical value. However, p*I* was increased in the range 5.75–5.90. In this case, multiple spots may represent differing isoforms, or modifications of the protein. Spot 126 was observed to have an extrapolated molecular mass of 219 100 Da with a p*I* of 5.4. One possibility is that this spot represents aggregation of α-actin 3 proteolytic fragments.

Spots 119, 120, 123–125 and 127 were identified as vinculin (theoretical mass/p*I* 116 600 Da/5.83). Spots 123–125 may represent vinculin isoforms and perhaps post-translational modifications. Again, poor resolution of large proteins in 2-DE may have prevented accurate estimation of vinculin molecular weight. The vinculin spots, however, exhibit increasing acidity. Again, phosphorylation may be suspected, as it has been demonstrated that vinculin is a substrate for serine/threonine and tyrosine kinases both *in vivo* and *in vitro* [32, 33]. Spots 119, 120 and 127 may be proteolytic fragments.

Spot 141 was identified as microfibril-associated glycoprotein 4 (theoretical mass/p*I* 28 600 Da/5.38). Observed values were calculated to be 37 300 Da/5.13. The probable cause of this significant increase in molecular weight is the post-translational addition of *N*- and/or *O*-linked

Table 1. Human saphenous vein smooth muscle protein spots identified by MALDI-TOF peptide mass fingerprinting (PMF) and nanospray-MS

Spot	Protein Identity	SWISS-PROT Entry name	SWISS-PROT Primary accession No.	Theoretical pI/mass Da (x 10^3)	Observed pI/mass Da (x 10^3)	% Sequence coverage
1	Unidentified	–	–	–	3.70/18.4	–
2	Calmodulin	CALM_HUMAN	P02593	4.09/16.7	3.80/16.1	46
3	Myosin light chain alkali (non-muscle isoform)	MLEN_HUMAN	P16475	4.56/16.8	4.14/15.7	77
4	Myosin light chain alkali (non-muscle isoform)	MLEN_HUMAN	P16475	4.56/16.8	4.26/15.5	77
5	Unidentified	–	–	–	4.05/22.3	–
6	Myosin regulatory light chain 2 (non-sarcomeric)	MLRM_HUMAN	P19105	4.67/19.7	4.58/21.2	31
7	Unidentified	–	–	–	4.65/19.7	–
8	Myosin regulatory light chain 2, smooth muscle isoform	MLRN_HUMAN	P24844	5.09/19.7	4.80/21.9	71
9	Unidentified	–	–	–	4.76/14.4	–
10	Galectin-1	LEG1_HUMAN	P09382	5.34/14.6	5.14/13.6	81
11	Unidentified	–	–	–	5.17/11.0	–
12	SH3 domain-binding glutamic acid-rich-like protein	SH3L_HUMAN	O75368	5.22/12.8	5.44/13.8	64
13	[Q]Tropomyosin beta chain, fibroblast and epithelial muscle-type	TPM2_HUMAN	P06468	4.63/33.0	5.25/17.8	20
14	Unidentified	–	–	–	5.21/19.6	–
15	Unidentified	–	–	–	5.22/20.7	–
16a	Actin	ACTC_HUMAN	P04270	5.23/42.0	4.95/20.2	28
16b	Actin	ACTC_HUMAN	P04270	5.23/42.0	4.89/18.7	29
17	Unidentified	–	–	–	5.52/18.7	–
18	Unidentified	–	–	–	5.62/18.0	–
19	SM22 alpha/transgelin (actin binding protein)	TAGL_HUMAN	Q01995	8.88/22.5	5.78/18.9	51
20	Unidentified	–	–	–	6.06/14.0	–
21	Unidentified	–	–	–	6.77/13.4	–
22	Haemoglobin beta chain	HBB_HUMAN	P02023	6.81/15.9	7.02/13.3	82
23	Unidentified	–	–	–	7.58/12.2	–
24	Haemoglobin alpha chain	HBA_HUMAN	P01922	8.73/15.1	8.48/12.6	91
25	SM22 alpha/transgelin (actin-binding protein)	TAGL_HUMAN	Q01995	8.88/22.5	7.92/14.4	70
26	Unidentified	–	–	–	8.36/18.2	–
27	Cofilin, non-muscle isoform (Cofilin 1)	COF1_HUMAN	P23528	8.22/18.5	7.81/18.5	62
28	Destrin (actin depolymerising factor)	DEST_HUMAN	P18282	8.06/18.5	7.55/17.4	56
29	Peptidyl-Prolyl cis-trans isomerase A	CYPH_HUMAN	P05092	7.82/17.9	7.48/17.0	67
30	Peptidyl-Prolyl cis-trans isomerase A	CYPH_HUMAN	P05092	7.82/17.9	7.16/17.3	74
31	Cofilin, Muscle isoform (Cofilin-2)	COF2_HUMAN	Q9Y281	7.66/18.7	6.97/19.3	55
32	SM22 alpha/transgelin (actin binding protein)	TAGL_HUMAN	Q01995	8.88/22.5	6.44/17.7	49
33	SM22 alpha/transgelin (actin binding protein)	TAGL_HUMAN	Q01995	8.88/22.5	6.42/18.7	38
34	SM22 alpha/transgelin (actin binding protein)	TAGL_HUMAN	Q01995	8.88/22.5	6.06/17.6	36
35	SM22 alpha/transgelin (actin binding protein)	TAGL_HUMAN	Q01995	8.88/22.5	6.05/19.0	62
36	SM22 alpha/transgelin (actin binding protein)	TAGL_HUMAN	Q01995	8.88/22.5	6.00/21.8	37
37	P20 protein	p20 protein-human	Gil1082675	5.95/17.1	6.05/21.8	86
38	SM22 alpha/transgelin (actin-binding protein)	TAGL_HUMAN	Q01995	8.88/22.5	6.19/21.7	45
39	SM22 alpha/transgelin (actin-binding protein)	TAGL_HUMAN	Q01995	8.88/22.5	6.64/22.1	74
40	Alpha-crystallin B chain	CRAB_HUMAN	P02511	6.76/20.2	6.89/23.5	66
41	SM22 alpha/transgelin (actin binding protein)	TAGL_HUMAN	Q01995	8.88/22.5	7.50/24.9	36
42	Transgelin 2	TAG2_HUMAN	P37802	8.41/22.4	7.93/25.0	82
43	SM22 alpha/transgelin (actin binding protein)	TAGL_HUMAN	Q01995	8.88/22.5	9.17/25.8	67
44	SM22 alpha/transgelin (actin binding protein)	TAGL_HUMAN	Q01995	8.88/22.5	9.90/26.2	51
45	SM22 alpha/transgelin (actin binding protein)	TAGL_HUMAN	Q01995	8.88/22.5	8.64/26.1	51
46	Peroxiredoxin 1 (thioredoxin-dependent peroxide reductase 2)	PDX1_HUMAN	Q06830	8.27/22.1	7.90/26.2	62
47	SM22 alpha/transgelin (actin binding protein)	TAGL_HUMAN	Q01995	8.88/22.5	7.57/26.1	39

Table 1. Continued

Spot	Protein Identity	SWISS-PROT Entry name	SWISS-PROT Primary accession No.	Theoretical pI/mass Da (x 10^3)	Observed pI/mass Da (x 10^3)	% Sequence coverage
48	Unidentified	–	–	–	6.93/25.9	–
49	Unidentified	–	–	–	6.67/24.9	–
50	SM22 alpha/transgelin (actin binding protein)	TAGL_HUMAN	Q01995	8.88/22.5	6.67/26.3	48
51	Triosephosphate isomerase	TPIS_HUMAN	P00938	6.51/26.5	6.60/29.1	43
52	Triosephosphate isomerase	TPIS_HUMAN	P00938	6.51/26.5	6.74/29.2	66
53	[Q]Ras suppressor protein 1	RSU1_HUMAN	Q15404	8.57/31.5	8.32/30.0	36
54	Galectin-3	LEG3_HUMAN	P17931	8.60/26.1	8.19/30.5	37
55	Ras suppressor protein 1 (by inspection)	RSU1_HUMAN	Q15404	8.57/31.5	7.60/30.0	34
56	Phosphoglycerate mutase, brain form	PMGB_HUMAN	P18669	6.75/28.7	6.70/29.9	64
57	Antioxidant protein 2	AOP2_HUMAN	P30041	6.02/24.9	6.19/29.8	59
58	Unidentified	–	–	–	6.09/27.3	–
59	Glutathione-S-Transferase P	GTP_HUMAN	P09211	5.44/23.2	5.60/27.6	91
60	Peroxiredoxin 2 (thioredoxin-dependent peroxide reductase 1)	PDX2_HUMAN	P32119	5.66/21.9	5.58/26.0	67
61	Unidentified	–	–	–	5.40/25.7	–
62	Rho GDP-dissociation inhibitor 1 (Rho GDI 1)	GDIR_HUMAN	P52565	5.03/23.2	5.08/29.7	38
63	Heat shock 27 kD protein (HSP 27)	HS27_HUMAN	P04792	7.83/22.3	5.45/29.9	52
64	Heat shock 27 kD protein (HSP 27)	HS27_HUMAN	P04792	7.83/22.3	5.62/29.9	72
65	Heat shock 27 kD protein (HSP 27)	HS27_HUMAN	P04792	7.83/22.3	6.02/29.8	58
66	Actin alpha skeletal muscle (aa 40–375, fragment)	ACTS_HUMAN	P02568	5.55/37.8	5.56/31.3	25
67	Chloride intracellular channel protein 1	CLI1_HUMAN	O00299	5.09/26.9	5.32/32.7	37
68	Actin alpha skeletal muscle (aa 40–375, fragment)	ACTS_HUMAN	P02568	5.55/37.8	5.47/33.9	24
69	F-actin capping protein alpha-2 subunit	CAZ2_HUMAN	P47755	5.57/32.9	5.66/37.1	65
70	Annexin IV	ANX4_HUMAN	P09525	5.85/35.8	5.81/34.5	42
71	Annexin V1 (lipocortin VI)	ANX6_HUMAN	P08133	5.42/75.7	6.14/36.1	21
72	Esterase D	ESTD_HUMAN	P10768	6.54/31.5	6.60/34.0	57
73	Glyceraldehyde 3-phosphate dehydrogenase, liver	G3P2_HUMAN	P04406	8.58/35.9	7.04/35.7	26
74	Calponin H1, smooth muscle (Basic calponin)	CLP1_HUMAN	P51911	9.14/33.2	9.08/35.7	30
75	Calponin H1, smooth muscle (Basic calponin)	CLP1_HUMAN	P51911	9.14/33.2	9.22/35.7	10
76	Calponin H1, smooth muscle (Basic calponin)	CLP1_HUMAN	P51911	9.14/33.2	9.50/35.9	34
77	Calponin H1, smooth muscle (Basic calponin)	CLP1_HUMAN	P51911	9.14/33.2	8.76/35.7	33
78	Calponin H1, smooth muscle (Basic calponin)	CLP1_HUMAN	P51911	9.14/33.2	8.49/35.7	21
79	Glyceraldehyde-3-phosphate dehydrogenase, liver	G3P2_HUMAN	P04406	8.58/35.9	8.32/37.2	57
80	Glyceraldehyde-3-phosphate dehydrogenase, liver	G3P2_HUMAN	P04406	8.58/35.9	7.98/37.4	36
81	[Q]Alpha-actinin-2 associated LIM protein	O60439	O60439	8.38/34.3	7.05/36.9	35
82	Alcohol dehydrogenase [NADP(+)]	ALDX_HUMAN	P14550	6.35/36.4	6.45/39.6	44
83a	L-lactate dehydrogenase H chain	LDHH_HUMAN	P07195	5.72/36.5	5.77/37.9	31
83b	Tropomyosin, fibroblast and epithelial muscle type	TPM2_HUMAN	P06468	4.63/32.9	5.77/37.9	40
84	Actin, gamma-enteric smooth muscle (alpha-actin 3)	ACTH_HUMAN	P12718	5.31/41.9	5.89/40.5	22
85	Actin, gamma-enteric smooth muscle (alpha-actin 3)	ACTH_HUMAN	P12718	5.31/41.9	5.90/41.7	22
86	LIM and SH3 domain protein-1	LAS1_HUMAN	Q14847	6.61/29.7	6.14/38.2	64
87	NEDD5 protein homolog	NED5_HUMAN	Q15019	6.15/41.5	6.17/41.7	42
88	Phosphoglycerate kinase 1	PGK1_HUMAN	P00558	8.30/44.6	7.70/41.7	41
89	Fructose-bisphosphate aldolase A	ALFA_HUMAN	P04075	8.39/39.3	7.90/40.2	66
90	Phosphoglycerate kinase 1	PGK1_HUMAN	P00558	8.30/44.6	8.00/41.6	50
91	Elongation factor 1-alpha 1	EF11_HUMAN	P04720	9.10/50.1	9.20/45.5	17
92	Prolargin [precursor]	PARG_HUMAN	P51888	9.47/43.8	8.30/51.4	27
93	Prolargin [precursor]	PARG_HUMAN	P51888	9.47/43.8	8.08/51.6	24
94	Pyruvate kinase, M1 isozyme	KPY1_HUMAN	P14618	7.57/57.7	7.52/55.3	47
95	Prolargin [precursor]	PARG_HUMAN	P51888	9.47/43.8	7.35/52.4	42
96	ATP synthase H+ transporting mitochondrial F1 complex alpha chain	ATPA_HUMAN	P25705	8.28/55.2	7.67/49.2	34

Table 1. Continued

Spot	Protein Identity	SWISS-PROT Entry name	SWISS-PROT Primary accession No.	Theoretical pI/mass Da (x 10^3)	Observed pI/mass Da (x 10^3)	% Sequence coverage
97	Integrin-linked protein kinase 1	ILK1_HUMAN	Q13418	8.30/51.4	7.54/47.3	24
98	Alpha enolase	ENOA_HUMAN	P06733	6.99/47.0	6.80/45.6	61
99a	[Q]Annexin XI	ANXA_HUMAN	P50995	5.20/37.2	7.03/52.7	21
99b	[Q]Prolargin [precursor]	PARG_HUMAN	P51888	9.47/43.8	7.03/52.7	28
100	Alpha enolase	ENOA_HUMAN	P06733	6.99/47.0	6.57/45.6	30
101	Annexin XI	ANXA_HUMAN	P50995	7.53/54.4	6.63/52.6	28
102	Aldehyde dehydrogenase, cytosolic	DHAC_HUMAN	P00352	6.29/54.7	6.19/52.4	39
103	Aldehyde dehydrogenase, mitochondrial X	DHA5_HUMAN	P30837	6.01/55.3	6.17/50.3	35
104	Aldehyde dehydrogenase, mitochondrial X [precursor]	DHA5_HUMAN	P30837	6.41/57.2	6.08/50.3	44
105	Unidentified	–	–	–	6.16/53.2	–
106	Dihydropyrimidinase related protein-3	DPY3_HUMAN	Q14195	6.04/62.0	6.08/56.5	22
107	Dihydropyrimidinase related protein-3	DPY3_HUMAN	Q14195	6.04/62.0	6.19/56.3	28
108	Aldehyde dehydrogenase, cytosolic	DHAC_HUMAN	P00352	6.29/54.7	6.38/51.8	31
109	Transforming growth factor-beta induced protein IG-H3 [precursor]	BGH3_HUMAN	Q15582	7.62/74.7	6.47/59.1	51
110	Transforming growth factor-beta induced protein IG-H3 [precursor]	BGH3_HUMAN	Q15582	7.62/74.7	6.69/58.6	31
111	Transforming growth factor-beta induced protein IG-H3 [precursor]	BGH3_HUMAN	Q15582	7.62/74.7	6.58/59.1	42
112	DJ1092A11.3 WD repeat domain 1	Q9NTK7	Q9NTK7	6.37/51.6	6.31/61.5	57
113	DJ1092A11.3 WD repeat domain 1	Q9NTK7	Q9NTK7	6.37/51.6	6.39/61.5	51
114	Aconitate hydratase, mitochondrial [precursor]	ACON_HUMAN	Q99798	7.36/85.4	7.03/85.7	26
115	Unidentified	–	–	–	6.73/136.0	–
116	Unidentified	–	–	–	6.61/135.5	–
117	Filamin	ABP_HUMAN	P21333	5.73/28.1	6.05/118.8	15
118	[Q]Filamin	ABP_HUMAN	P21333	5.73/28.1	6.03/120.0	13
119	Vinculin	VINC_HUMAN	P18206	5.83/116.6	6.05/134.1	12
120	Vinculin	VINC_HUMAN	P18206	5.83/116.6	6.02/134.9	25
121	Gelsolin (actin depolymerization factor)	GELS_HUMAN	P06396	5.90/85.7	5.83/93.7	21
122	Gelsolin (actin depolymerization factor)	GELS_HUMAN	P06396	5.90/85.7	5.74/94.1	41
123	Vinculin	VINC_HUMAN	P18206	5.83/116.6	5.72/182.2	24
124	Vinculin	VINC_HUMAN	P18206	5.83/116.6	5.65/173.7	18
125	Vinculin	VINC_HUMAN	P18206	5.83/116.6	5.60/174.8	18
126	Actin, gamma-enteric smooth muscle (alpha-actin 3)	ACTH_HUMAN	P12718	5.31/41.9	5.43/219.1	31
127	Vinculin	VINC_HUMAN	P18206	5.83/116.6	5.44/111.5	16
128	Heat shock cognate 71 kDa protein	HS7C_HUMAN	P11142	5.37/70.9	5.48/64.6	42
129	Heat Shock 70 kDa protein 1	HS71_HUMAN	P08107	5.48/70.1	5.54/63.3	53
130	Protein disulphide isomerase ER-60	PDA3_HUMAN	P30101	5.61/54.3	5.80/53.7	38
131	Actin, gamma-enteric smooth muscle (alpha-actin 3)	ACTH_HUMAN	P12718	5.31/41.9	5.75/42.3	51
132	Actin, gamma-enteric smooth muscle (alpha-actin 3)	ACTH_HUMAN	P12718	5.31/41.9	5.76/41.6	38
133	Creatine kinase B chain	KCRB_HUMAN	P12277	5.34/42.6	5.59/42.5	70
134	Actin, gamma-enteric smooth muscle (alpha-actin 3)	ACTH_HUMAN	P12718	5.31/41.9	5.53/42.7	34
135	Beta tubulin	TBB2_HUMAN	P05217	4.79/49.8	5.50/37.4	39
136	Osteoinductive factor [precursor] (OIF)	OIF_HUMAN	P20774	5.46/33.9	5.27/35.9	19
137	Osteoinductive factor [precursor] (OIF)	OIF_HUMAN	P20774	5.46/33.9	5.26/36.9	26
138	Annexin V	ANX5_HUMAN	P08758	4.94/35.8	5.01/34.8	33
139	Tropomyosin, fibroblast	TPM4_HUMAN	P07226	4.67/28.5	4.50/33.4	24
140	Tropomyosin beta chain, fibroblast and epithelial muscle-type	TPM2_HUMAN	P06468	4.63/33.0	4.53/38.7	17
141	Microfibril-associated glycoprotein 4	MFA4_HUMAN	P55083	5.38/28.6	5.13/37.3	45
142	Actin, gamma-enteric smooth muscle (alpha-actin 3)	ACTH_HUMAN	P12718	5.31/41.9	5.44/43.5	67
143	Gamma enolase	ENOG_HUMAN	P09104	4.94/47.2	4.92/46.5	32

Table 1. Continued

Spot	Protein Identity	SWISS-PROT Entry name	SWISS-PROT Primary accession No.	Theoretical pI/mass Da (x 10^3)	Observed pI/mass Da (x 10^3)	% Sequence coverage
144	ATP synthase beta chain, mitochondrial [precursor]	ATPB_HUMAN	P06576	5.26/56.6	5.11/49.2	52
145	Tropomyosin, fibroblast and epithelial muscle-type	TPM2_HUMAN	P06468	4.63/33.0	4.60/46.6	40
146	Calreticulin [precursor]	CRTC_HUMAN	P27797	4.29/48.1	4.11/65.7	23
147	78 kDa glucose-regulated protein [precursor]	GR78_HUMAN	P11021	5.03/72.1	5.09/74.1	29
148	Alpha actin, aortic smooth muscle	ACTA_HUMAN	P03996	5.24/42.0	5.37/105.9	28
149	Alpha-1 collagen VI (aa 574–1009)(fragment)	Q14040	Q14040	5.52/47.9	5.27/181.2	45

Protein identification from a two-dimensional gel of human saphenous vein medial smooth muscle (Fig. 1). Protein identity, primary SWISS-PROT/TrEMBL accession number or GenBank number, percentage coverage and observed and theoretical p*I*/mass are indicated. Superscript 'Q' indicates protein spot identity confirmed by nanospray-MS.

glycan oligosaccharide chains. This has previously been demonstrated to retard the migration of glycoprotein SDS polyacrylamide gels [34].

Spots 63–65 were identified as the 27 000 Da heat shock protein, HSP27. The shift in p*I* observed in this case is indicative of change in protein charge associated with varying degrees of phosphorylation. HSP27 has four major phosphorylation isoforms: non-, mono-, di- and tri-phosphorylated, exhibiting an accompanying increase in acidity. Armstrong and colleagues [35] demonstrated that HSP27 from adult rabbit cardiomyocytes can be resolved as eight isoelectric isoforms. Scheler *et al.* [36] were able to demonstrate fifty-nine isoelectric isoforms of HSP27 with twelve spots changing in dilated cardiomyopathy in the p*I* range of 4.9–6.2 and mass range of 27 000–28 000 Da. In this study we have identified three distinct isoforms exhibiting increasing degrees of acidity (p*I* values 6.02, 5.62 and 5.45, spots 65, 64 and 63, respectively).

Spots 73, 79 and 80 were identified as glyceraldehyde 3-phosphate dehydrogenase (GAPDH, theoretical mass/p*I* 35 900 Da/8.58). Of the three spots, 79 and 80 form a charge train of molecular masses 37 200 and 37 400 Da with p*I* values of 8.32 and 7.98, respectively. Here, there is an obvious increase in GAPDH acidity. Phosphorylation of GAPDH has been demonstrated in rabbit muscle [37], porcine brain [38] and a human liver cell line [39]. It is likely then, that spots 79 and 80 are GAPDH molecules in various degrees of phosphorylation, spot 80 being more highly phosphorylated than 79. Spot 73 was further identified as a liver isoform of the protein, but may be a proteolytic fragment, as evidenced by its lower molecular mass and p*I* (35 700 Da/7.04)

MALDI-MS analysis of spot 83 revealed two distinct spectra. This would initially indicate that two protein spots had comigrated at indistinguishable molecular weight and p*I* positions. This phenomenon may occur when proteins are separated under low resolution conditions (*i.e.* pH 3–10 gradients). In this case spot 83 was identified as L-lactate dehydrogenase H-chain (83a) and tropomyosin (83b). However, the observed p*I* value obtained for spot 83b of 5.77 appeared to be substantially more basic than the value obtained for the vast majority of tropomyosin identified (spot 140). A possible explanation for this is that during IEF a "smearing" effect of tropomyosin has occurred which may be due to the particular abundance of this protein.

Two spots were identified as proteins of non-smooth muscle cell origin. Analysis revealed that spots 22 and 24 were haemoglobin β and α chains, respectively. The probable source of these contaminants is the saphenous vein microvasculature, which cannot be easily removed from our medial layer dissections. However, these very abundant erythrocyte proteins constitute less than 2% of total proteins identified.

Twenty protein spots were not identified. This in part may have been due to an insufficient amount of protein in the spot, despite pooling from replicate gels. Low molecular weight proteins may also compound this difficulty due to scarcity of tryptic digest sites. Indeed, 8 of the 20 unidentified spots ranged in molecular mass from 11 000 Da to 18 700 Da. However, the possibility remains that some unidentified protein spots may be novel and therefore not described in published databases.

4 Concluding remarks

The map of protein expression we have generated will be a useful tool in the identification and quantification of proteins, which may be differentially expressed, modified or regulated in HSV bypass vessels. In addition this map could be of use in investigating other pathologies centred around vascular smooth muscle cells. The map may also

facilitate the comparison of protein expression in smooth muscle cells of varying origins, and be used to relate protein expression to the various roles of these subtypes.

We thank the Graham Dixon Trust (Charing Cross), the British Heart Foundation, and the Charing Cross Special Trustees for financial support, and thank Jules A. Westbrook (Heart Science Centre, Harefield Hospital) for his technical help in running two-dimensional gels. RW thanks the Wellcome Trust for purchase of the MALDI spectrometer and SYW is grateful to the Medical Research Council for financial support.

Received April 30, 2001

5 References

[1] Nwasokwa, O. N., *Ann. Intern. Med.* 1995, *123*, 528–545.
[2] Motwani, J. G., Topol, E. J., *Circulation* 1998, *97*, 916–931.
[3] McCollum, C. N., Alexander, C., Kenchingtn, G., Franks, P. J., Greenhalgh, R. M., *J. Vasc. Surg.* 1991, *13*, 150–162.
[4] Davies, M. G., Hagen, P. O., *Br. J. Surg.* 1994, *81*, 1254–1269.
[5] Hsu, S. M., Raine, L., Fanger, H., *J. Histochem. Cytochem.* 1981, *29*, 577–580.
[6] Weekes, J., Wheeler, C. H., Yan, J. X., Weil, *et al.*, *Electrophoresis* 1999, *20*, 898–906.
[7] Heinke, M. Y., Wheeler, C. H., Yan, J. X., Amin, V., *et al.*, *Electrophoresis* 1999, *20*, 2086–2093.
[8] Bradford, M. M., *Anal. Biochem.* 1976, *72*, 248–254.
[9] Rabilloud, T., Valette, C., Lawrence, J. J., *Electrophoresis* 1994, *15*, 1552–1558.
[10] Sanchez, J.-C., Rouge, V., Pisteur, M., Ravier, F., *et al.*, *Electrophoresis* 1997, *18*, 324–327.
[11] Görg, A., Boguth, G., Obermaier, C., Posch, A., Weiss, W., *Electrophoresis* 1995, *16*, 1079–1086.
[12] Görg, A., Postel, W., Weser, J., Günther, S., *et al.*, *Electrophoresis* 1987, *8*, 122–124.
[13] Anderson, N. L., *Two-Dimensional Electrophoresis: Operation of the ISO-DALT System*, Large Scale Biology Press, Washington DC 1988.
[14] Yan, J. X., Wait, R., Berkelman, T., Harry, R. A., *et al.*, *Electrophoresis* 2000, *21*, 3666–3672
[15] Jeno P., Mini, T., Moes, S., Hintermann, E., Horst, M., *Anal. Biochem.* 1995, *224*, 75–82.
[16] Wilm, M., Shevchenko, A., Houthaeve, T., Breit, S., *et al.*, *Nature* 1996, *379*, 466–469.
[17] Shevchenko, A., Wilm, M., Vorm, O., Mann, M., *Anal. Chem.* 1996, *68*, 850–858.
[18] Gharahdaghi, F., Weinberg, C. R., Meagher, D. A., Imai, B. S., Mische, S. M., *Electrophoresis* 1999, *20*, 601–605.
[19] Vorm, O., Mann, M., *J. Am. Soc. Mass Spectrom.* 1994, *5*, 955–958.
[20] Perkins, D. N., Pappin, D. J., Creasy, D. M., Cottrell, J. S., *Electrophoresis* 1999, *20*, 3551–3567.
[21] Zhang, W., Chait, B. T., *Anal. Chem.* 2000, *72*, 2482–2489.
[22] Altschul, S. F., Madden, T. L., Schäffer, A. A., Zhang, J., *et al.*, *Nucleic Acids Res.* 1997, *25*, 3389–3402.
[23] Amersham Pharmacia Biotech Brochure no. 18–1140–60. *Immobiline DryStrip Visualisation of pH gradients*.
[24] Rabilloud, T., Adessi, C., Giraudel, A., Lunardi, J., *Electrophoresis* 1997, *18*, 307–316.
[25] Gimona, M., Sparrow, M. P., Strasser, P., Herzog, M., Small, J. V., *Eur. J. Biochem.* 1992, *205*, 1067–1075.
[26] Erdodi, F., Rokolya, A., Barany, M., Barany, K., *Arch. Biochem. Biophys.* 1988, *266*, 583–591.
[27] Lees-Miller, J. P., Heeley, D. H., Smillie, L. B., Kay, C. M., *J. Biol. Chem.* 1987, *262*, 2988–2993.
[28] Takahashi, K., Nadal-Ginard, B., *J. Biol. Chem.* 1990, *266*, 13284–13288.
[29] Kwiatkowski, D. J., *Curr. Opin. Cell Biol.* 1999, *11*, 103–108.
[30] Sun, H., Yamamoto, M., Mejillano, M., Yin, H. L., *J. Biol. Chem.* 1999, *274*, 33179–33182.
[31] Moon, A., Drubin, D. G., *Mol. Biol. Cell.* 1995, *6*, 1423–1431.
[32] Werth, D. K., Niedel, J. E., Pastan, I., *J. Biol. Chem.* 1983, *258*, 11423–11426.
[33] Sefton, B. M., Hunter, T., Ball, E. H., Singer, S. J., *Cell* 1981, *24*, 165–174.
[34] Poduslo, J. F., *Anal. Biochem.* 1981, *114*, 131–139.
[35] Armstrong, S. C., Delacey, M., Ganote, C. E., *J. Mol. Cell. Cardiol.* 1999, *31*, 555–567.
[36] Scheler, C., Li, X., Salnikow, J., Dunn, M. J., Jungblut, P. R., *Electrophoresis* 1999, *20*, 3623–3628.
[37] Kawamoto, R. M., Caswell, A. H., *Biochemistry* 1986, *25*, 657–661.
[38] Wu, K., Aoki, C., Elste, A., Rogalski-Wilk, A. A., Siekevitz, P., *Proc. Natl. Acad. Sci. USA.* 1997, *94*, 13273–13278.
[39] Duclos-Vallee, J. C., Capel, F., Mabit, H., Petit, M. A., *J. Gen. Virol.* 1998, *79* ,1665–1670.